(1)

ARMY RESEARCH LABORATORY

Mechanical Behavior of 97.2% W Alloy In Tension at High Temperatures

John L. Green

ARL-TR-508

September 1994

Approved for public release; distribution unlimited.

The findings in this report are not to be construed as an official Department of the Army position unless so designated by other authorized documents.

Citation of manufacturer's or trade names does not constitute an official endorsement or approval of the use thereof.

Destroy this report when it is no longer needed. Do not return it to the originator.

REPORT DOCUMENTATION PAGE

Form Approved
OMB No. 0704-0188

1. AGENCY USE ONLY (Leave blank)	2. REPORT DATE	3. REPORT TYPE AND DATES COVERED
	September 1994	Final Report

4. TITLE AND SUBTITLE
Mechanical Behavior of 97.2% W Alloy in Tension at High Temperatures

5. FUNDING NUMBERS

6. AUTHOR(S)
John L. Green

7. PERFORMING ORGANIZATION NAME(S) AND ADDRESS(ES)
U.S. Army Research Laboratory
Watertown, MA 02172-0001
ATTN: AMSRL-MA-PD

8. PERFORMING ORGANIZATION REPORT NUMBER
ARL-TR-508

9. SPONSORING/MONITORING AGENCY NAME(S) AND ADDRESS(ES)
U.S. Army Research Laboratory,
2800 Powder Mill Road
Adelphi, MD 20783-1197

10. SPONSORING/MONITORING AGENCY REPORT NUMBER

11. SUPPLEMENTARY NOTES

12a. DISTRIBUTION/AVAILABILITY STATEMENT
Approved for public release; distribution unlimited.

12b. DISTRIBUTION CODE

13. ABSTRACT (Maximum 200 words)

The objective was to investigate the behavior of 97.2% tungsten alloy in tension. A modified button head specimen was heated using resistive heating techniques. The affect high temperatures, medium strain rates, and heating rates had on the stress-strain results were observed. A high speed optical pyrometer and an optical clip gage were utilized for temperature and strain measurements. The optical clip gage could measure strain at strain rates up to 11.8 s^{-1}. The room temperature experiments were at strain rates of 10^{-4} s^{-1}, 10^{-2} s^{-1}, and 5 s^{-1}. The high heating rate experiments were at temperatures of 727°C, and 1097°C, heating rates of 5.4°C/sec and 536°C/sec and a strain rate of 5 s^{-1}. Increase in yield point and flow stress were observed as the heating rate was increased. A modified Johnson - Cook (MJ+C) material model was proposed to include the effect of heating rate. The constants in the MJ+C model were determined based on the experimental results.

14. SUBJECT TERMS
Tungsten, High temperatures, Strain rate, Material modeling

15. NUMBER OF PAGES
20

16. PRICE CODE

17. SECURITY CLASSIFICATION OF REPORT	18. SECURITY CLASSIFICATION OF THIS PAGE	19. SECURITY CLASSIFICATION OF ABSTRACT	20. LIMITATION OF ABSTRACT
Unlimited	Unlimited	Unlimited	UL

Contents

Figures

Tables

Introduction

The objective of this report was to investigate the effect of high heating rates on a 97.2% W alloy, and compare the experimental results to the Johnson-Cook (J+C) [1] material model. Rapid heating, high temperatures, and triaxial stress states are experienced by all materials involved in the armor penetration process. Laboratory experiments are conducted to gain an understanding of how a material responds to these types of conditions. These experiments provide information on target failure and ballistic performance of the materials involved (i.e., V_{50} and Depth of Penetration data [2]). Ballistic test results do not yield mechanical properties of armor/anti-armor materials. This mechanical property data is required for conducting computer simulations of these ballistic events. The data can only be acquired from controlled laboratory experiments (ie. tension, compression and torsion tests). These experiments measure the mechanical responses such as load and deformation which can change with various loading rates, temperatures, and heating rates. The experimental results are used to gain an understanding of a material's behavior, and obtain constants for mathematical material models used in computer simulations of an event. Most experimental data is acquired at strain rates between 10^{-4} s^{-1} and 10,000 s^{-1}, and at various isothermal temperatures up to the materials melting point. Investigators have researched the affect heating rate has on a material's properties and observed that the rate of heating can alter a materials stress strain relation [3], [4]. These observations have never been incorporated into a material model, and the role heating rate has on materials involved in armor/anti-armor interactions have never been considered in computer simulations. Since the material model dose not include the high heating rate effect, the engineer must adjust the model's constants to force the simulation to agree with the real event (i e., ballistic penetration simulation). Therefore a material model that includes the heating rate effect should provide more accurate simulations of events that combine rapid heating and high temperatures.

To determine if heating rate alters the stress strain relation of the W alloy a series of high temperature and heating rate experiments were conducted. The W alloy specimens were heated and tested at temperatures between 25°C to 1097°C, and heating rates of 5.4°C/sec, and 536°C/sec, also isothermal experiments were conducted to provide a baseline condition that the heating rate experiments could be compared to. Room temperature tension specimens were loaded to failure at strain rates of 10^{-4} s^{-1}, 10^{-2} s^{-1}, and 5 s^{-1}. The high heating rate test process consisted of the following; immediately upon achieving test temperature the specimen was then loaded in tension to failure at a strain rate of 5 s^{-1}. For the isothermal test the specimen was held at test temperature for 5 minutes before loading to failure at a strain rate of 5 s^{-1}. The data acquired from measurements of load, strain, temperature and time were used to generate stress strain relations at different heating rates, strain rates and temperatures.

To model the W alloy stress-strain results the (J+C) material model was choosen. This is an uncoupled model, therefore any necessary modification can be easily accomplished. The J+C model's constants for the W alloy were obtained from the room temperature and high temperature isothermal experimental results. The J+C model does not have a term that accounts for changes in stress magnitude due to the rate of material heating. Therefore it became necessary to modify the J+C model. A modified Johnson-Cook (MJ+C) material model was proposed that included the effect of heating rate. This MJ+C model has an additional term with one additional constant. The additional term is a logrithmic function

that will increase the magnitude of stress with increasing heating rate. The constant for this term is "G", and was determined based on the high heating rate experimental results.

Material and Specimen Design

The specimens tested were made of a 97.2% W alloy. This heavy metal alloy was manufactured by Kennametal, the manufacturer's name is W2. Its large weight-to-volume ratio make it an ideal candidate material for static and dynamic applications (i.e. perpetrators, and shape charge liners). The W alloy is a powder metallurgy product of tungsten, nickel, and iron. The chemical composition, mechanical and electrical properties are listed in Tables 1 and 2, respectively.

Table 1. Chemical Composition of 97.2% W Alloy

Material	W	Ni	Fe	Cu	Co
W2	97.2%	1.5%	0.7%	0.5%	0.1%

Table 2. Mechanical and Electrical Properties of 97.2% W Heavy Metal Alloy

Tensile Strength (MPa)	827.4
Yield Strength (0.2% Offset)	*
Modulus of Elasticity (GPa)	358.5
Elongation (%)	9
Poisson's Ratio	0.27
Hardness (Rockwell C)	27 to 32
Density (g/cc)	18.5
Electrical Conductivity, % IACS	31.0
Electrical Resistivity, ohms-m	5.5×10^{-8}
Permeability	1×10^{-6}
Total Emissivity at 1500 C	0.23

* Not available from manufacturer's data sheets

A modified button head specimen was employed. The angle of specimen's bearing surface was changed from 15° to 70° relative to centerline, and the outside diameter of button head was increased from 1.27 cm to 2.54 cm. This larger bearing surface was necessary to keep button head from plastically deforming at high temperatures. The specimen gage section dimensions are the same as standard button head specimen. The diameter of specimen's gage length was chosen to eliminate the possibility of skin effects during heating. The heating apparatus, fixtures and specimen were designed to give uniform heating of the specimen, for a more detailed explanation see Reference 2.

Experimental Procedure

All specimens were tested in tension. The test were conducted at three temperatures, three strain rates, and three heating rate conditions in accordance to Table 3. This test plan provided a set of data that clearly displays the affect that temperature, strain rate, and heating rate have on the tungsten alloy.

Table 3. 97.2% W alloy Test Matrix

Test Temperature (°C)	Strain Rate (s^{-1})	Heating Rate (°C/sec)	Number of Tests
25	10^{-4}	isothermal	4
25	10^{-2}	isothermal	4
25	5	isothermal	4
727	5	isothermal	1
727	5	5.4	2
727	5	536	2
1097	5	[illegible]	2

Specimen testing was conducted in the Medium Strain Rate Machine (MSRM), at strain rates of 10^{-4} s^{-1}, 10^{-2} s^{-1}, and 5 s^{-1}. The MSRM machine has two operating modes: the closed loop mode and the open loop mode. In the closed loop mode, the MSRM behaves like a typical servo-hydraulic controlled test machine. A strain/load/displacement rate up to 1 sec^{-1} can be achieved in closed loop mode. In the open loop mode, the hydraulic fluid is replaced by nitrogen gas. A fast-acting valve is used to release the gas from the top or bottom of an actuating piston creating a pressure differential which moves the piston. The loading rate in the open loop mode is controlled by the gas pressure, piston stroke, and fast acting valve orifice size, strain rates up to 50 s^{-1} can be achieved. A computer and a digital oscilloscope were used to control the MSRM and record the data.

The heating apparatus utilized resistance heating. This method involves passing current through the specimen, and the specimen's resistance converts the current to heat. The apparatus consists of a Variac auto transformer which controls the power output of the apparatus. A step down transformer converted low current high voltage to high current low voltage. A schematic of heating apparatus is shown in Figure 1.

The high voltage on/off relay operation is controlled by the computer's digital input/output signals. The system is actuated by a command in the test program to trigger the relay and allow the current to flow through the specimen. The desired heating rate for a particular specimen geometry and material can be obtained by adjusting the voltage and measuring the temperature and time history.

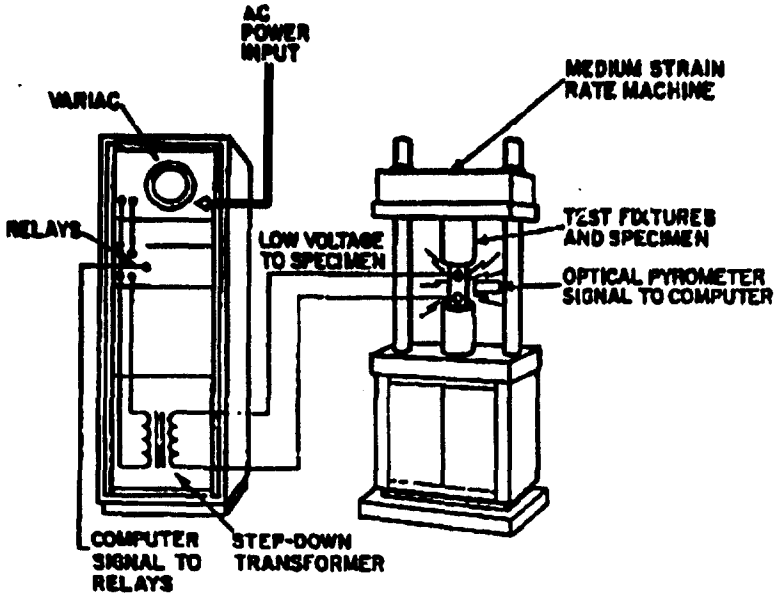

Figure 1. Schematic of high heating rate apparatus.

The specimen temperature was measured with a pyrometer that had a response time of 5 milliseconds and linear temperature response between the temperatures 460°C to 1650°C. The pyrometer was calibrated by placing a 97.2% W specimen in a inert atmosphere with a type K thermocouple attached. The pyrometer was focused on the specimen as it was slowly heated. The output from pyrometer was calibrated with output from thermocouple, the calibration equation is

$$Y = -0.3821 + 0.00108(X) \qquad (1)$$

where Y is the pyrometer output in units of volts, and X is the thermocouple output in units of °C. The calibration equation has a correlation coefficient of 0.9961. Figure 2 is a plot of pyrometer output (volts) versus thermocouple output (°C).

When alternating current (ac) is passed through metals, the possibility of skin effects must be examined. Skin effects occur when current is alternating back and forth. The internal effects tend to force the current to flow in the outer portion of the conductor [5]. For tungsten with a resistivity of 5.5×10^{-8} ohms-m, The (diameter) thickness beyond which the skin effect is significant is 1.7 cm. This is greater than the specimen's diameter of 0.635 cm, therefore skin effects should not affect the uniformity of specimen heating.

One of the most difficult problems encountered in high temperature mechanical testing is the measurement of strains, especially at dynamic loading conditions. The maximum temperature which can be sustained by the foil strain gages is around 270°C. High temperature weld able strain gages can survive at temperatures up to 1400°C but are limited to maximum of 0.5% strain, and their cost is

prohibitive. Clip gages and extensometers constitute alternate measuring techniques. These devices are mechanically fragile and must be removed prior to specimen failure. Furthermore, the maximum response time of ordinary extensometers is about 10 Hz which is much too slow for the high strain rate test. A laser has been utilized in the optical tracking method [6] which requires attaching two flags to the specimen as targets. The disadvantage is that at large plastic deformations, the targets could be out of range of the viewport. A second type of laser extensometer utilizes a dual frequency laser beam and the natural diffraction which occurs on specimen surface [7], the draw back is it's limited ability to measure at maximum strain rate of 1 s^{-1}.

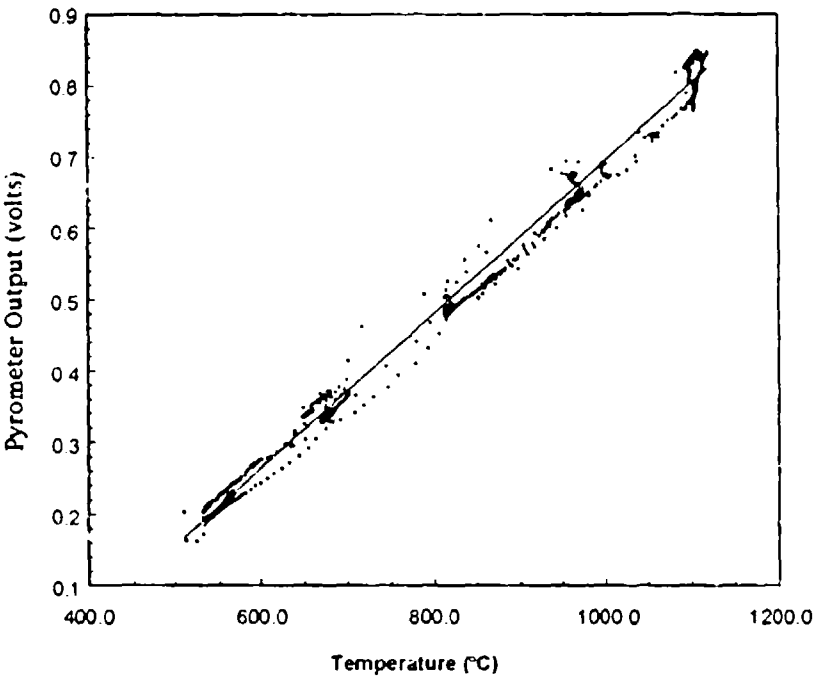

Figure 2. Pyrometer calibration curve of 97.2% W specimen in an inert atmosphere.

Since there were no extensometers available that could meet the requirements of being able to withstand high temperatures, with ability to measure at strain rates of 5 s^{-1}., and reasonable cost, a special optical extensometer was designed and built. This device is based on the detection of changes in light intensity. The variation from a diffraction pattern is sensed by an optical switch that outputs an electrical impulse, and then recorded. Figure 3 is a schematic of the output from the optical extensometer and the load cell. The extensometer's calibration is $2.15 \times 10^{-4} \pm 8.7 \times 10^{-6}$ cm from peak-to-peak. The optical switch has a rise time of six microseconds. This enables the extensometer to operate at a maximum strain rate of 11.8 s^{-1}.

The lenses are mounted in sliders with ceramic knife edges as shown in Figure 4. To maintain proper alignment and contact, a second set of sliders is mounted opposite the first set. Spring loaded tie bolts connect opposite sliders and provide clamping action. Ceramic knife edges secure the sliders to the specimen and also provide thermal and electric isolation from the gage.

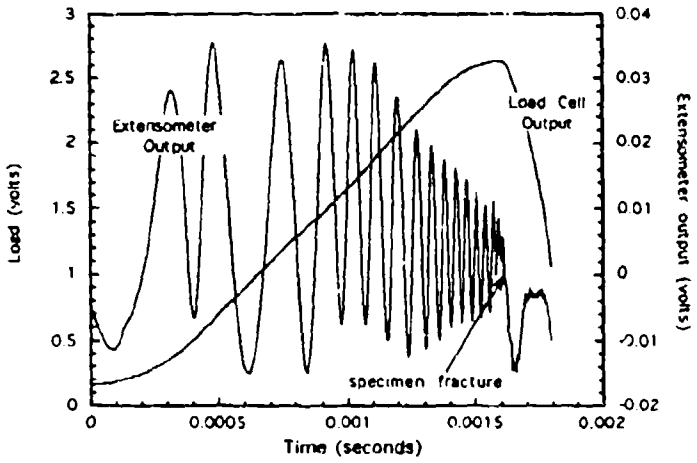

Figure 3. Typical extensometer and load cell output signals.

The gage length is represented by the initial distance between knife edges. At fracture, the sliders separate and each half remains attached to its portion of the specimen. Reassemble requires simply slipping the two haives together.

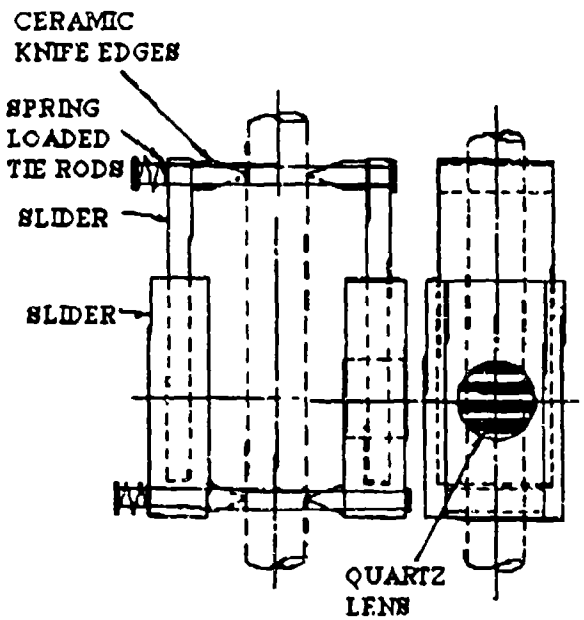

Figure 4. Schematic of optical clip gage attached to specimen.

Discussion of Experimental Results and Modeling

This section discusses the experimental results and the modified Johnson-Cook material model. From the stress-strain curves at various strain rates, temperatures and heating rates, failure stress, failure strain, 0.2% offset yield point, and the modulus of elasticity were obtained. A summary of results are in Table 4.

Table 4. Average Mechanical Properties of 97.2% W Alloy at Various Strain Rates

Number of Tests	Strain Rate (sec^{-1})	Temperature (°C)	Heating Rate (°C/sec)	Average Failure Stress MPa	Average Failure Strain (%)	Average 0.2% Offset Yield Point MPa	Average Modulus of Elasticity GPa
4	10^{-4}	25	isothermal	1110	1.0	1106	378
5	10^{-2}	25	isothermal	1230	0.9	1248	359
4	5	25	isothermal	1500	0.6	1490	372
2	5	727	isothermal	250	0.58	240	81
2	5	727	5.4	229	0.57	250	90
2	5	727	536	378	0.67	367	82
2	5	1097	536	143	0.44	150	71

The stress-strain curves were plotted for each set of specimens using average data, to exam the effect of strain rate, heating rate, and temperature. The affect of strain rate is displayed in Figure 5 for the room temperature isothermal specimens, the "X" symbols denote specimen failure. The specimens were tested in tension at three strain rates, 10^{-4} s^{-1}, 10^{-1} s^{-1}, and 5 s^{-1}. Increase in the strain rate from 10^{-4} s^{-1} and 5 s^{-1} increased the yield point from 1106 MPa to 1490 MPa, respectively. The same increase in strain rate caused an increased failure stress of 35%. The strain at failure decreased from 1% to 0.6% for an increase in strain rate from 10^{-4} s^{-1} to 5 s^{-1}. In the next set of experiments different temperatures were used, but the heating rate and strain rate were held constant at 536°C/sec and 5 s^{-1}, respectively. The results of these experiments are shown in Figure 6. As the temperature increased the yield point and failure stress decreased, at a temperature of 727°C the yield point was 367 MPa. This decreased to 150 MPa with an increase in temperature to 1097°C.

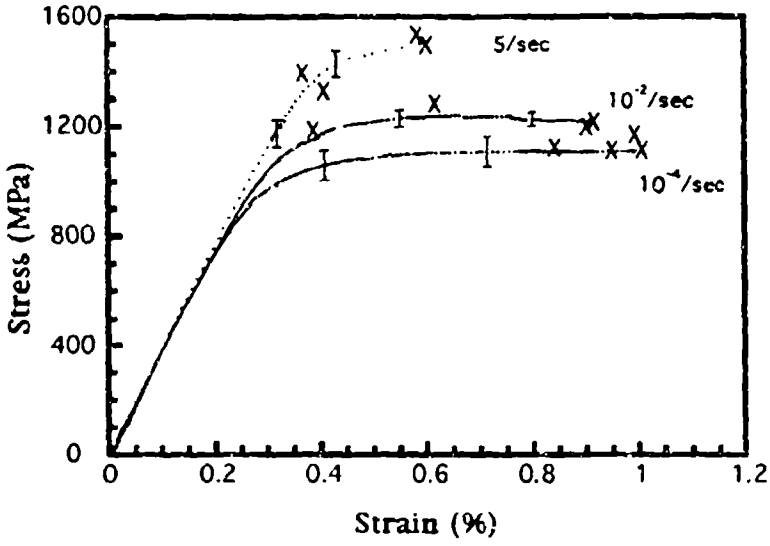

Figure 5. Average stress-strain results for 97.2% W alloy at 25°C, displaying effect of strain rate.

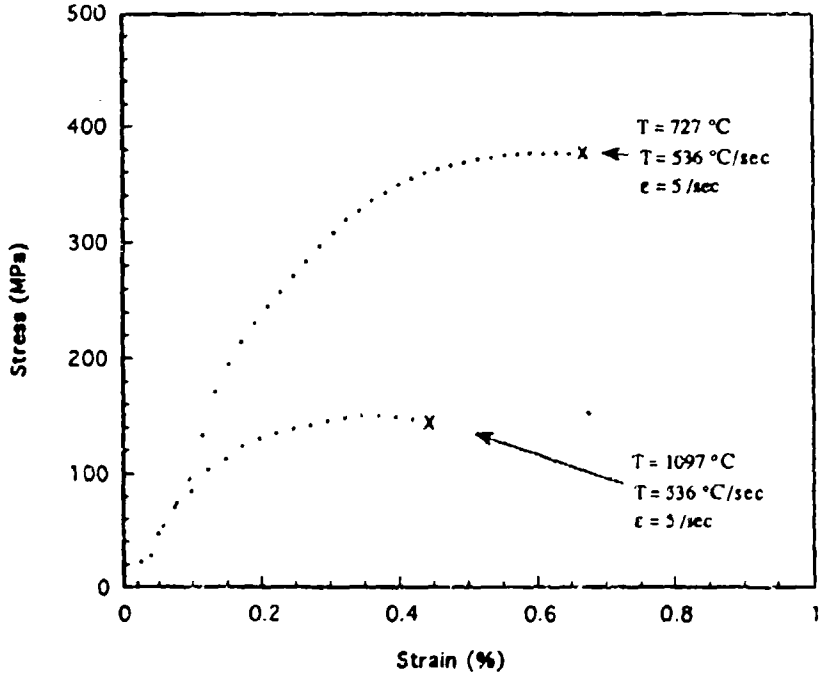

Figure 6. Effect of temperature on 97.2% W alloy at a constant strain rate and heating rate.

The heating rate effect is displayed in Figure 7. The temperature and strain rate were held constant at 727°C and 5 s^{-1}, respectively. Three heating rate conditions were, isothermal, 5.4°C/sec and 536°C/sec. For the same temperature and strain rate the yield stress for isothermal and 5.4°C/sec experiments were almost the same, 240 MPa and 250 MPa, respectively. For a heating rate of 536°C/sec the yield stress increased to 372 MPa. The strain at failure and the modulus of elasticity were not significantly affected by the heating rate.

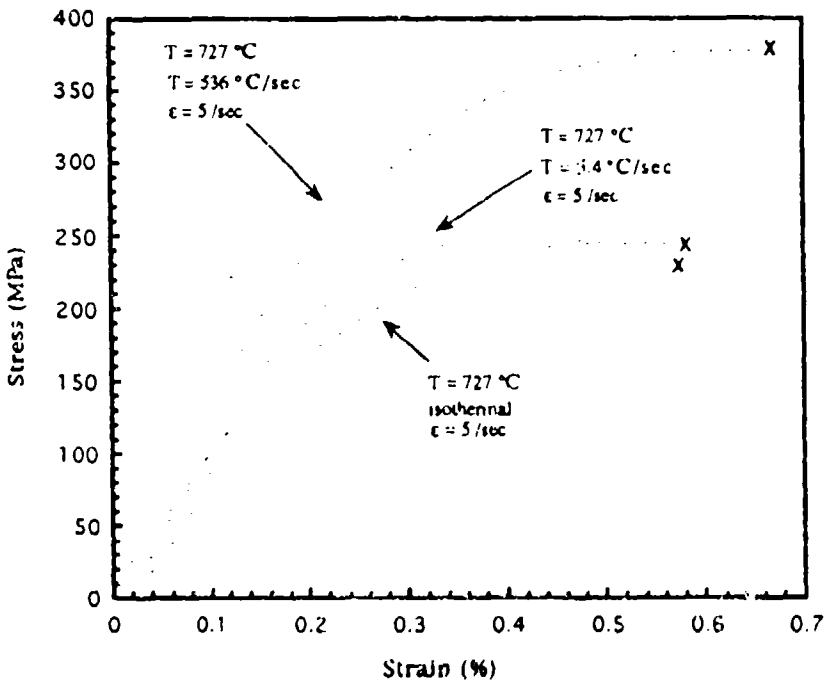

Figure 7. Effect of heating rate on 97.2% W alloy at 727°C and strain rate of 5 sec^{-1}

These results indicated that for small heating rates i.e., 5.4°C/sec yield stresses and flow stresses do not increase, but for larger heating rates of 536°C/sec there is an increas in yield stresses and failure stresses. Using these sets of data the effects of strain rate, heating rate and temperature were modeled. The Johnson-Cook (J+C) material model was chosen because it is an uncoupled model with strain rate and temperature terms, therefore a heating rate term can easily be included. The form of Johnson-Cook is:

$$\sigma = (A + B\,\varepsilon^{n})(1 + C \ln\dot{\varepsilon})(1-((T-T_{room}) / (T_{melt}-T_{room}))^{m}) \qquad (2)$$

where:
A = 1400 MPa
B = 1500 MPa
n = 0.7
C = 0.014
m = 0.1

These five constants were experimentally determined from the results in this study and compression results on same material from Reference 8. The melting temperature of the nickel-iron-tungsten matrix material was choosen for T_{melt} [9] The value for T_{melt} is 1525°C The affect of heating rate is not accounted for by the Johnson-Cook model. Therefore the model must be modified to account for the high heating rate effect Since the effect of heating rate is similar to strain rate, (increase in strain rate or heating rate yields increase in stress), and because the limited experimental data acquired indicates a logarithmic relation between heating rate and yield stress, an equation similar to the strain rate term was used The heating rate term is.

$$1 + (G * \ln(1+\dot{T})) \qquad (3)$$

where "G" is the heating rate constant in units of sec/°C, and the heating rate is $\dot{T}$ is in units of °C/sec The heating rate term changes the material's calculated stress as a function of rate of temperature change At low heating rates the calculated stress would not be changed, but as the heating rate is increased the heating rate term would be greater than one and this would cause an increase in the calculated stress The modified Johnson-Cook(MJ+C) model has the following form,

$$\sigma = (A + B\,\varepsilon^{n})(1 + C\ln\dot{\varepsilon})(1-((T-T_{room}) / (T_{melt}-T_{room}))^{m}) \\ (1 + (G * \ln(1+\dot{T}))) \qquad (4)$$

where the six constants are

A = 1400 MPa
B = 1500 MPa
n = 0 7
C = 0 014
m = 0.1
G = 0 08 sec/°C

To obtain the value for "G" the model was fitted to the high heating rate plastic stress-strain results at 727°C with a heating rate of 536°C/s The high heating rate and isothermal results at a temperature of 727°C along with the MJ+C model results are in Figure 8 By adding the heating rate term with a value of 0 08 for "G" the MJ+C model duplicates the plastic experimental results very well The Johnson-Cook model is only used to model the plastic behavior of material, therefore the elastic part of stress strain curve is not used in fitting the MJ+C model

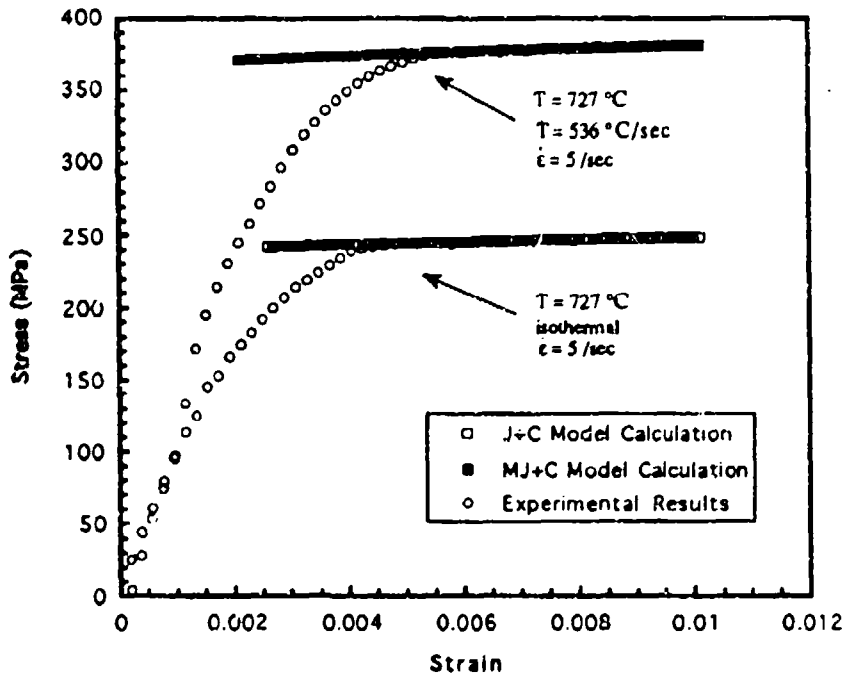

Figure 8. Isothermal and 536°C/sec heating rate experimental and model results at a temperature of 727°C, and strain rate of 5 s^{-1}.

To test how well the MJ+C model accounts for the stress increase due to heating rate, the model was compared with other experimental data at different heating rates, temperatures and strain rates.

Figure 6 displays data at a heating rate of 536°C/sec and various temperatures and Figure 7 has data at various heating rates and a temperature of 727°C. Using these sets of data the MJ+C model can be tested. For the case of a high heating rate at different temperatures, the comparison of experimental data and MJ+C model is in Figure 9. The two test temperatures were 727°C, and 1097°C. The MJ+C model was calibrated with the 727°C test ("G" constant was obtained from that test data), therefore experiment and MJ+C model should compare very well. The other data set was the test case. The magnitude of stress in the 1097°C test was less than the MJ+C model prediction. The difference in flow stress between experimental and model results at a strain of 0.003 strain was 25 MPa. This diference is attributed to inacuracies in the J+C model temperature term [10]. More experiments and modification of the temperature term will be required to eliminate these differences in flow stress between model and experimental results.

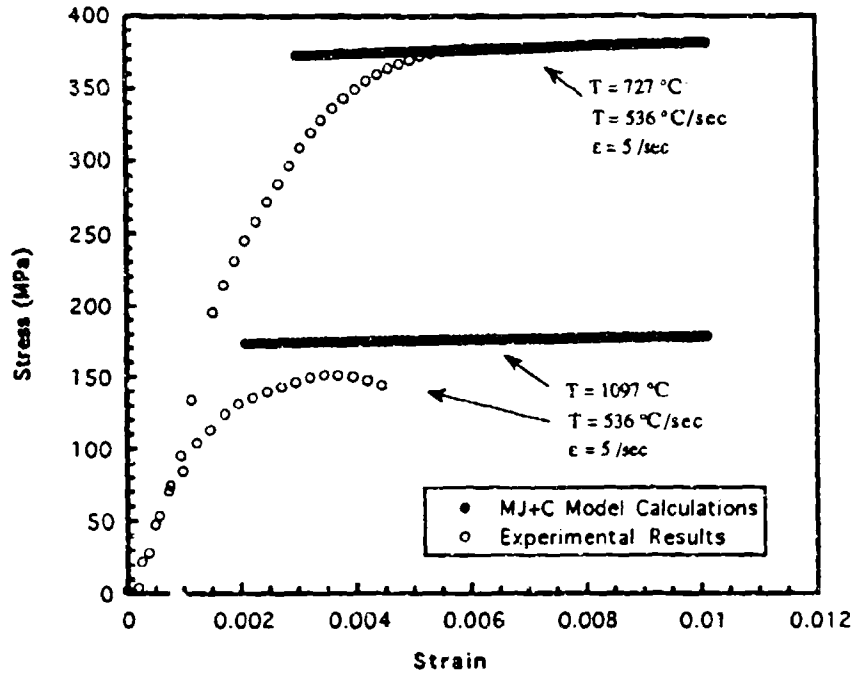

Figure 9. Comparison of MJ+C model and experimental data at various temperatures, heating rate of 536°C/sec, and strain rate of 5 s^{-1}.

The model was applied to data from tests conducted at same temperature and strain rate with different heating rates. There were two heating rates used 5.4°C/sec and 536°C/sec. The 536°C/sec data set was used to calibrate the MJ+C model. The model was tested on the 5.4°C/sec. The model predicted the magnitude of flow stress at 0.004 strain very well, as shown in Figure 10. The model does not simulate the drop off in stress magnitude beyond 0.004 strain. This decrease in stress magnitude can not be explained at this time.

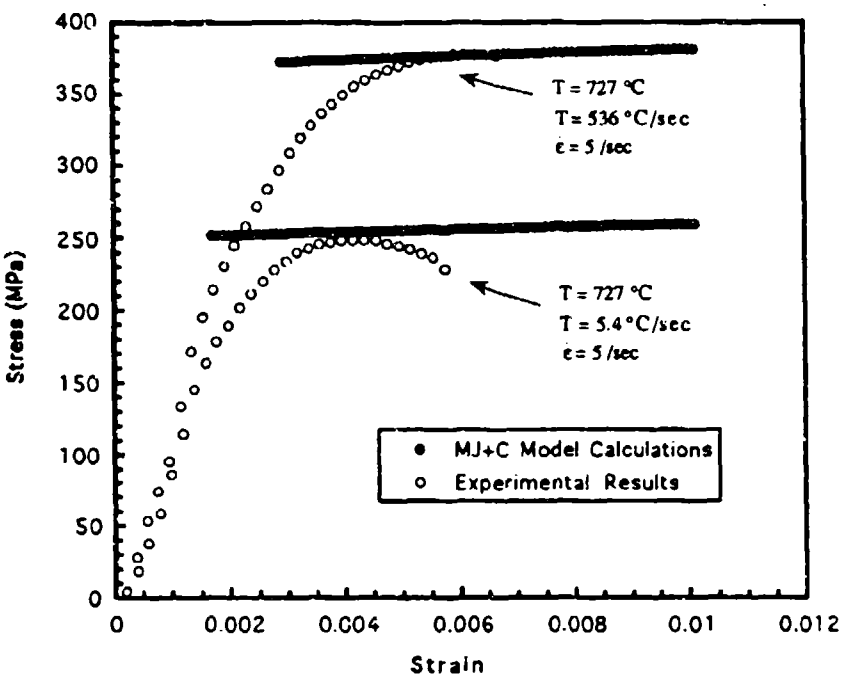

Figure 10. Comparison of MJ+C model and experimental data at various heating rates, temperature of 727°C, and strain rate of 5 s^{-1}.

Conclusions

Tension stress-strain data was acquired at strain rates between 10^{-4} s^{-1} to 5 s^{-1}, temperatures between 25°C (room temperature) and 1097°C, heating rates of 5.4°C/sec and 536°C/sec and isothermal conditions. There is clear indication from results that this material is sensitive to strain rate, heating rate and temperature. A modified Johnson-Cook material model was proposed to include the effect of heating rate. The constants in the modified Johnson-Cook model (MJ+C) were determined based on the experimental results. This model accounts for the effects of strain rate, heating rate and temperature. Although the MJ+C model tested well at different heating rates, it only tested fair to diferent test temperatures. To resolve the inaccuracies in model predictions more experiments and further modification of MJ+C will be required. The constants in MJ+C material model are applicable only for the strain rate, heating rate and temperature ranges used in this study.

Acknowledgments

The author thanks Messrs P. Moy and S. Romeo for assisting in specimen testing and data analysis. The author also thanks Mr. W. Crenshaw, Mr. W. Bethoney, Dr. D. P. Dandekar, and Dr. T. Weerasooriya, for valuable technical discussions and support in this study.

References

1. Dowqing, R. J., Tauer, K. J., Woolsey, P., and Hodi, F. S. The Metallurgical and Ballistic Characterization of Quarter-Scale Tungsten Alloys Penetrators. U.S. Army Research Laboratory, MTL TR 90-91, May 1990.

2. Chou, S. C., and Green, J. L. Mechanical Behavior of SiC/2014 Al Composite at High Temperature. Advanced Composite Materials and Structures Proceedings, G. C. Shi and S. E. Hsu, eds.,1986

3. Babcock, S. G., Langan, J. J., Norvey, D. B., Michaels, T. E., Schierloh, F. L., and Green, S. J. Characterization of Three Aluminum Alloys. U.S. Army Research Laboratory, AMMRC CR 71-3, January 1971.

4. Johnson, G. R., and Cook, W. H. A Constitutive Model and Data for Metals Subjected to Large Strains, High Strain Rates and High Temperatures., Proceedings of the Seventh International Symposium on Ballistics., The Hague, The Netherlands 1983 p 541-547.

5. Smythe, W. R. Static and Dynamic Electricity, Third Edition, McGraw-Hill, New York, 1968.
6. Marion, R. H., A New Method of High-Temperature Strain Measurement, Experimental Mechanics, Vol. 18, No. 4, April 1978, p 134-140,.

7. Hercher, M., Wyntjes, G., and DeWeerd, H. Non-Contact Laser Extensometer, Proceedings of SPIE, vol 746, Industrial Laser Interferometry, January 1987, p 185-191.

8. Green, J. L., and Moy, P. Large Strain Compression of Two Tungsten Alloys at Various Strain Rates. U.S. Army Research Laboratory, MTL TR 92-66, September 1992.

9. Winslow, F. R. The Nickel-Iron-Tungsten Phase Diagram. Y-12 Plant Report No. 1785, Oak Ridge, Tennessee, 1971.

10 Weerasooriya, T., and Moy, P. Deformation Behavior of 93W-5Ni-2Fe at Different Dates of Dompression Loading and Temperatures, to be published as ARL report.

DISTRIBUTION LIST

No. of Copies	To
1	Office of the Under Secretary of Defense for Research and Engineering, The Pentagon, Washington, DC 20301
	Director, U.S. Army Research Laboratory, 2800 Powder Mill Road, Adelphi, MD 20783-1197
1	ATTN: AMSRL-OP-SD-TP, Technical Publishing Branch
1	AMSRL-OP-SD-TA, Records Management
1	AMSRL-OP-SD-TL, Technical Library
	Commander, Defense Technical Information Center, Cameron Station, Building 5, 5010 Duke Street, Alexandria, VA 23304-6145
2	ATTN: DTIC-FDAC
1	MIA/CINDAS, Purdue University, 2595 Yeager Road, West Lafayette, IN 47905
	Commander, Army Research Office, P.O. Box 12211, Research Triangle Park, NC 27709-2211
1	ATTN: Information Processing Office
	Commander, U.S. Army Materiel Command, 5001 Eisenhower Avenue, Alexandria, VA 22333
1	ATTN: AMCSCI
	Commander, U.S. Army Materiel Systems Analysis Activity, Aberdeen Proving Ground, MD 21005
1	ATTN: AMXSY-MP, H. Cohen
	Commander, U.S. Army Missile Command, Redstone Arsenal, AL 35809
1	ATTN: AMSMI-RD-CS-R/Doc
	Commander, U.S. Army Armament, Munitions and Chemical Command, Dover, NJ 07801
1	ATTN: Technical Library
	Commander, U.S. Army Natick Research, Development and Engineering Center Natick, MA 01760-5010
1	ATTN: SATNC-MI, Technical Library
	Commasnder, U.S. Army Satellite Communications Agency, Fort Monmouth, NJ 07703
1	ATTN: Technical Document Center
	Commander, U.S. Army Tank-Automotive Command, Warren, MI 48397-5000
1	ATTN: AMSTA-ZSK
1	AMSTA-TSL, Technical Library
	President, Airborne, Electronics and Special Warfare Board, Fort Bragg, NC 28307
1	ATTN: Library
	Director, U.S. Army Research Laboratory, Weapons Technology, Aberdeen Proving Ground, MD 21005-5066
1	ATTN: AMSRL-WT

No. of Copies	To
	Commander, Dugway Proving Ground, UT 84022
1	ATTN: Technical Library, Technical Information Division
	Commander, U.S. Army Research Laboratory, 2800 Powder Mill Road, Adelphi, MD 20783
1	ATTN: AMSRL-SS
	Director, Benet Weapons Laboratory, LCWSL, USA AMCCOM, Watervliet, NY 12189
1	ATTN: AMSMC-LCB-TL
1	AMSMC-LCB-R
1	AMSMC-LCB-RM
1	AMSMC-LCB-RP
	Commander, U.S. Army Foreign Science and Technology Center, 220 7th Street, N.E., Charlottesville, VA 22901-5396
3	ATTN: AIFRTC, Applied Technologies Branch, Gerald Schlesinger
	Commander, U.S. Army Aeromedical Research Unit, P.O. Box 577, Fort Rucker, AL 36360
1	ATTN: Technical Library
	U.S. Army Aviation Training Library, Fort Rucker, AL 36360
1	ATTN: Building 5906-5907
	Commander, U.S. Army Agency for Aviation Safety, Fort Rucker, AL 3636
1	ATTN: Technical Library
	Commander, Clarke Engineer School Library, 3202 Nebraska Ave., N., Fort Leonard Wood, MO 65473-5000
1	ATTN: Library
	Commander, U.S. Army Engineer Waterways Experiment Station, P.O. Box 631, Vicksburg, MS 39180
1	ATTN: Research Center Library
	Commandant, U.S. Army Quartermaster School, Fort Lee, VA 23801
1	ATTN: Quartermaster School Library
	Naval Research Laboratory, Washington, DC 20375
1	ATTN: Code 6384
	Chief of Naval Research, Arlington, VA 22217
1	ATTN: Code 471
	Commander, U.S. Air Force Wright Research and Development Center, Wright-Patterson Air Force Base, OH 45433-6523
1	ATTN: WRDC/MLLP, M. Forney, Jr.
1	WRDC/MLBC, Mr. Stanley Schulman
	U.S. Department of Commerce, National Institute of Standards and Technology, Gaithersburg, MD 20899
1	ATTN: Stephen M Hsu, Chief, Ceramics Division, Institute for Materials Science and Engineering

No. of Copies	To
1	Committee on Marine Structures, Marine Board, National Research Council, 2101 Constitution Avenue, N.W., Washington, DC 20418
1	Materials Sciences Corporation, Suite 250, 500 Office Center Drive, Fort Washington, PA 19034
1	Charles Stark Draper Laboratory, 555 Technology Square, Cambridge, MA 02139
	Wyman-Gordon Company, Worcester, MA 01601
1	ATTN: Technical Library
	General Dynamics, Convair Aerospace Division, P.O. Box 748, Fort Worth, TX 76101
1	ATTN: Mfg. Engineering Technical Library
	Plastics Technical Evaluation Center, PLASTEC, ARDEC, Bldg. 355N, Picatinny Arsenal, NJ 07806-5000
1	ATTN: Harry Pebly
1	Department of the Army, Aerostructures Directorate, MS-266, U.S. Army Aviation R&T Activity - AVSCOM, Langley Research Center, Hampton, VA 23665-5225
1	NASA - Langley Research Center, Hampton, VA 23665-5255
	U.S. Army Vehicle Propulsion Directorate, NASA Lewis Research Center, 2100 Brookpark Road, Cleveland, OH 44135-3191
1	ATTN: AMSRL-VP
	Director, Defense Intelligence Agency, Washington, DC 20340-6053
1	ATTN: ODT-5A, Mr. Frank Jaeger
	U.S. Army Communications and Electronics Command, Fort Monmouth, NJ 07703
1	ATTN: Technical Library
	U.S. Army Research Laboratory, Electronic Power Sources Directorate, Fort Monmouth, NJ 07703
1	ATTN: Technical Library
	Director, U.S. Army Research Laboratory, Watertown, MA 02172-0001
2	ATTN: AMSRL-OP-WT-IS, Technical Library
5	Author